

The Bifurcated Age-Metallicity Relation of Milky Way Globular Clusters and its Implications For the Accretion History of the Galaxy

Ryan Leaman^{1,2*}, Don A. Vandenberg³, and J. Trevor Mendel⁴

¹*Instituto de Astrofísica de Canarias, E-38205 La Laguna, Tenerife, Spain,* ²*Dept. Astrofísica, Universidad de La Laguna, E-38205 La Laguna, Tenerife,*

³*Dept. of Physics & Astronomy, University of Victoria, P.O. Box 3055, Victoria, B.C., V8W 3P6, Canada,* ⁴*Max-Planck-Institut für extraterrestrische*

Accepted 2013 August 14. Received 2013 May 17

ABSTRACT

We use recently derived ages for 61 Milky Way (MW) globular clusters (GCs) to show that their age-metallicity relation (AMR) can be divided into two distinct, parallel sequences at $[\text{Fe}/\text{H}] \gtrsim -1.8$. Approximately one-third of the clusters form an offset sequence that spans the full range in age ($\sim 10.5\text{--}13$ Gyr), but is more metal rich at a given age by ~ 0.6 dex in $[\text{Fe}/\text{H}]$. All but one of the clusters in the offset sequence show orbital properties that are consistent with membership in the MW disk. They are not simply the most metal-rich GCs, which have long been known to have disk-like kinematics, but they are the most metal-rich clusters at all ages. The slope of the mass-metallicity relation (MMR) for galaxies implies that the offset in metallicity of the two branches of the AMR corresponds to a mass decrement of 2 dex, suggesting host galaxy masses of $M_* \sim 10^{7-8} M_\odot$ for GCs that belong to the more metal-poor AMR. We suggest that the metal-rich branch of the AMR consists of clusters that formed in-situ in the disk, while the metal-poor GCs were formed in relatively low-mass (dwarf) galaxies and later accreted by the MW. The observed AMR of MW disk stars, and of the LMC, SMC and WLM dwarf galaxies are shown to be consistent with this interpretation, and the relative distribution of implied progenitor masses for the halo GC clusters is in excellent agreement with the MW subhalo mass function predicted by simulations. A notable implication of the bifurcated AMR, is that the identical mean ages and spread in ages, for the metal rich and metal poor GCs are difficult to reconcile with an in-situ formation for the latter population.

Key words: Galaxy: formation – (Galaxy:) globular clusters: general – galaxies: dwarf.

1 INTRODUCTION

The properties of globular cluster (GC) systems in disk and elliptical galaxies provide an opportunity not only to study the formation of these dense star clusters, but also to probe the dynamics, chemical evolution, and assembly history of their host galaxies (e.g., Pota et al. 2013). In our own Milky Way (MW), the GCs have long been used to support different scenarios for the mass growth of the stellar halo. For instance, the fact that the distribution of cluster metallicities does not vary significantly with Galactocentric distance (R_G) in GCs beyond $R_G \sim 8$ kpc was used in early work by Searle & Zinn (1978) to argue against the monolithic collapse model for the formation of the MW envisioned by Eggen, Lynden-Bell & Sandage (1962).

As most GCs are relatively simple stellar populations that formed nearly instantaneously, their ages are an even more useful property for investigating such scenarios. This is complicated, however, by the long-standing difficulty of determining accurate relative (let alone absolute) ages for GCs (e.g., compare the sometimes discordant results reported by Rosenberg et al. 1999, Vandenberg 2000, De Angeli et al. 2005, Marín-Franch et al. 2009). On the one hand, current predictions of turnoff luminosity versus age relations should be quite accurate given the steady improvement in the basic physics ingredients of stellar models (such as opacities and nuclear reaction rates) and the incorporation of diffusive processes that are thought to be important in the evolution of old, metal-deficient stars. On the other hand, it is still very risky to place a similar reliance on detailed fits of isochrones to the observed colour-magnitude diagrams (CMDs) of GCs because the predicted T_{eff} and colour scales have significant

* E-mail: rleaman@iac.es

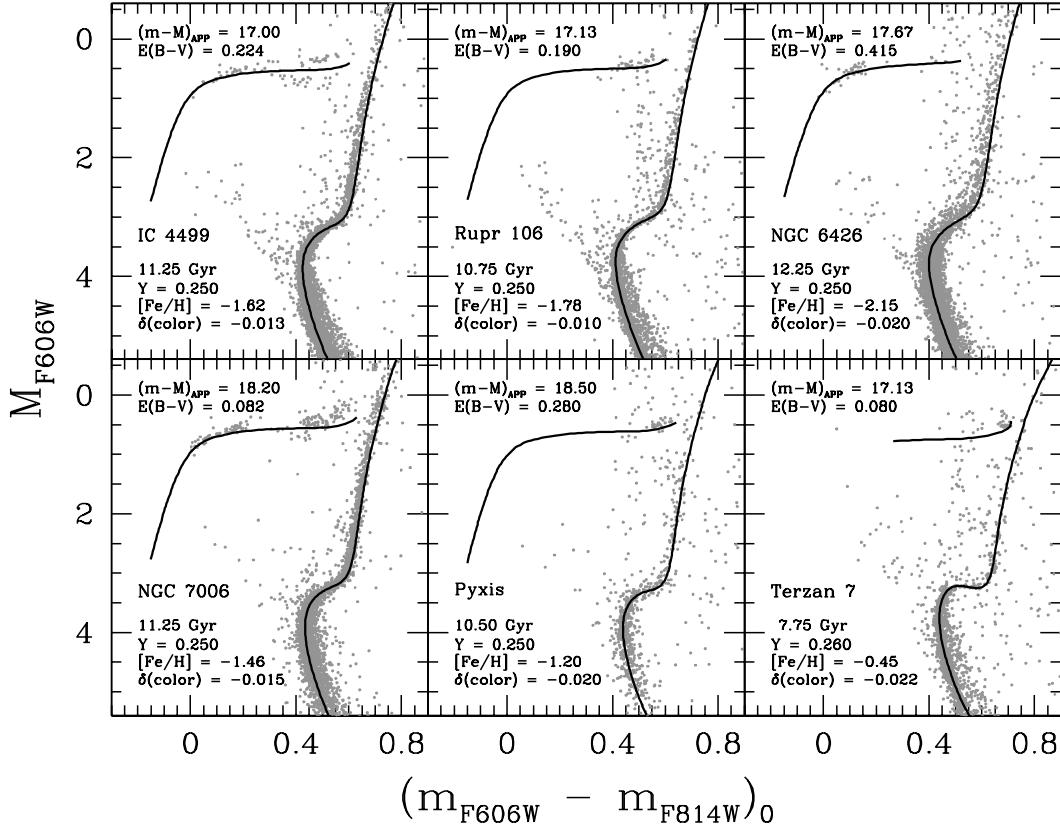


Figure 1. CMDs of six outer halo globular clusters, along with the best fitting isochrones following the method described in the text and V13. Each panel lists the adopted reddenings and apparent distance moduli that were found by fitting the ZAHB to the lower bound of the HB stars, along with the derived age. In addition, the assumed helium and $[\text{Fe}/\text{H}]$ values, as well as the adjustment in colour that was needed in order for the isochrone to match the observed turnoff colour are noted.

uncertainties associated with them (due to inadequacies in, e.g., the treatment of super-adiabatic convection and the atmospheric boundary condition). Although distance information is generally not needed when estimating relative GC ages, the latter do depend on the assumed $[\text{Fe}/\text{H}]$ values and any cluster-to-cluster variations that happen to be present in the abundances of helium, oxygen, and/or other α -elements (see VandenBerg et al. 2013, hereafter V13, see sections 5.3 and 6.1.1). In fact, it has become quite clear from recent observational studies that such variations exist (e.g., Carretta et al. 2009b), coupled with various chemical abundance anticorrelations and bimodalities, and that they account for some of the peculiar CMD morphologies which have been discovered (see the review by Gratton, Carretta & Bragaglia 2012).

The latest investigation of GC ages, by V13, employed an improved version of the classic ΔV_{TO}^{HB} method, which uses the magnitude difference between the horizontal branch (HB) and the turnoff (TO) as the primary age constraint. The main advantage of this technique over all others that have been proposed is that the effects of metal abundance uncertainties are minimized — because the luminosity of the HB and of the turnoff, at a fixed age, are both reduced when the metallicity is increased (and vice versa), although not by exactly the same amount. In addition, V13 used what appears to be a particularly robust way of determining the age once the absolute magnitude scale had been set by matching

a theoretical zero-age horizontal branch (ZAHB) locus for the latest estimate of the cluster metallicity (from Carretta et al. 2009a) to the lower bound of the observed distribution of its HB stars. Because the predicted variation of $M_V(\text{HB})$ with $[\text{Fe}/\text{H}]$ is in very good agreement with empirical determinations (see V13), the age-metallicity relation (AMR) that was derived in that study should be especially reliable. Interestingly, that AMR gives the visual impression of being bifurcated at $[\text{Fe}/\text{H}] \gtrsim -1.8$, such that clusters with halo-type or disk-like orbits populate different branches. In this paper, the V13 AMR has been augmented by data for six additional outer-halo GCs (with $15 \leq R_G \leq 40$ kpc), and after carrying out an examination of the kinematic properties of the GCs in the two sequences, we explore some the implications of the split AMR for the assembly of the MW.

2 GLOBULAR CLUSTER AGE DATA

We rely on the ages that V13 recently derived for the 55 Galactic GCs that they considered (based on photometry from Sarajedini et al. 2007), along with their adopted $[\text{Fe}/\text{H}]$ values (from the compilation given by Carretta et al. 2009a). Since similar *HST* Advanced Camera for Surveys (ACS) photometry has recently become available for a few additional outer-halo GCs (Dotter, Sarajedini & Anderson

2011)¹ we decided to take this opportunity to determine their ages using exactly the same procedure and stellar models that were employed by V13, and to include them in the AMR that is the subject of this investigation. Figure 1 illustrates the adopted fits of ZAHB models to the cluster HB stars and of isochrones to the turnoff (TO) portions of the observed CMDs. Reference should be made to V13 for a thorough discussion of the fitting procedure, but the main point to be emphasized here is that the age of each cluster is based on the fit of isochrones only to the observations in the vicinity of the turnoff (i.e., to the stars that have colours within $\simeq 0.05$ mag of the TO colour), where the morphology of the isochrones is predicted to be independent of the age and nearly independent of $[\text{Fe}/\text{H}]$, $[\alpha/\text{Fe}]$, helium abundance and the mixing-length parameter.

The indicated colour adjustments have been applied to the isochrones merely to demonstrate that they accurately reproduce the photometry both just above and just below the observed turnoffs and, therefore, that they have the same TO luminosities as observed. Such adjustments, regardless of whether they are due to errors in the model temperatures or the colour transformations, in the photometric zero-points, or in the assumed reddenings, have no impact on the derived ages. As found by V13, the red-giant branches (RGBs) of the best-fit isochrones tend to lie slightly to the red of the cluster giants, which suggests that the model temperatures or the adopted colour- T_{eff} relations or the assumed metallicities are not quite right. It is also possible that they are due, in part, to errors in the luminosities of the ZAHB models, since fainter ZAHBs would imply older ages and reduced TO-to-RGB colour differences. However, V13 derived ages of 13.0 Gyr for several of the GCs, and a significant upward revision of their ages is unlikely given that the age of the universe is 13.77 ± 0.06 Gyr (Bennett et al. 2012). This is a moot point anyway since we are much more interested in the differences in the ages of the GCs than in their absolute ages.

A few comments should be made concerning Figure 1. First, even though Palomar 15 was included in the Dotter, Sarajedini & Anderson (2011) data set, we decided against deriving an age for this system because it has a very blue HB along with a high and presumably uncertain reddening ($E(B - V) = 0.387$, according to Schlegel, Finkbeiner & Davis 1998), which make any fit of ZAHB models to the cluster HB population very uncertain. Second, with one exception (see the next paragraph), the adopted $[\text{Fe}/\text{H}]$ values were taken from the study by Carretta et al. (2009a) whenever possible. If the latter did not provide a metallicity estimate for a given cluster, we opted to use the $[\text{Fe}/\text{H}]$ value listed for it in the catalogue of cluster properties by Harris (2010). Third, reddenings identical to, or within 0.02 mag of, those given by Schlegel et al. were assumed, though higher or smaller values of $E(B - V)$ by ≈ 0.06 mag were adopted in the case of NGC 6426 and Pyxis, respectively, in order to obtain reasonably consistent interpretations of their CMDs. As reported by V13, the isochrones generally seem to predict TO colours that are too red by ~ 0.01 – 0.025 mag; consequently, we arbitrarily set the $\delta(\text{colour})$ values for these two GCs to be -0.02 mag and then adjusted their redden-

ings by the amounts needed to achieve satisfactory matches to both the TO and HB stars. Because the ZAHB loci are nearly horizontal where the HB stars in these two clusters are located, the impact of this approach on the derived ages is quite small ($\leq \pm 0.25$ Gyr).

Note that, whereas V13 did not attempt to determine an age for Terzan 7 because the Carretta et al. (2009a) metallicity for it ($[\text{Fe}/\text{H}] = -0.12$) was outside of the range for which stellar models were available, a closer examination leads us to suspect that such a high value of $[\text{Fe}/\text{H}]$ is unlikely to be correct. According to the Schlegel, Finkbeiner & Davis (1998) dust maps, the line-of-sight reddening in the direction of Ter 7 is 0.100 mag, and the absorbing gas/dust must be mostly in the foreground given that this GC has $R_G = 15.6$ kpc (Harris 2010). The intrinsic TO colour implied by this reddening suggests that the cluster metallicity must be significantly less than -0.12 . In fact, several spectroscopic studies (see Pritzl, Venn & Irwin 2005, and references therein) have obtained $[\text{Fe}/\text{H}] \approx -0.6$, as compared with the value of -0.32 that is given in the Harris catalogue. We therefore chose to adopt $[\text{Fe}/\text{H}] = -0.45$ as a compromise of those determinations, and because this estimate also leads to good agreement between the predicted and observed RGB slopes. In addition, we adopted $[\alpha/\text{Fe}] = 0.0$ (e.g., Tautvaišienė et al. 2004), which appears to be typical of other $[\text{Fe}/\text{H}] \gtrsim -1$ GCs that are associated with the Sagittarius dwarf galaxy (such as Pal 12, see Cohen 2004).

The other GCs considered in Figure 1 were assumed to have normal $[\alpha/\text{Fe}]$ values for their metallicities (see V13) in view of the results reported by, for instance, Smecker-Hane & McWilliam (2002) and Mottini, Wallerstein & McWilliam (2008). Although some studies (e.g., Brown, Wallerstein & Zucker 1997, Pritzl, Venn & Irwin 2005) found $[\alpha/\text{Fe}] \simeq 0.0$ for Ruprecht 106, they also reported $[\text{Fe}/\text{H}]$ values that are 0.3–0.4 dex higher than the value ($[\text{Fe}/\text{H}] = -1.78$) given by Carretta et al. (2009a). If the lower metallicity is more accurate, as we have assumed, then Ruprecht 106 has α -element abundances that are not too different from other GCs that have similar $[\text{Fe}/\text{H}]$ values. Further work is clearly needed to put the metallicities of Ruprecht 106 and other GCs that have been subjected to limited spectroscopic work, such as NGC 6426 and Pyxis, on a much firmer footing. However, such uncertainties do not have major consequences for ages based on the ΔV_{TO}^{HB} method because of its reduced sensitivity to the abundances of the heavy elements (as already noted). Indeed, the random uncertainties of our age estimates are within $\sim \pm 0.25$ – 0.5 Gyr: it is quite apparent from Figure 1 that isochrones for our best estimates of the cluster ages generally provide quite agreeable fits to the observed CMDs.

Finally we include the intriguing metal-rich open cluster NGC 6791, and adopt the average metallicity and derived age from the detailed study of (Brogaard et al. 2012), which used stellar evolutionary models and methodology consistent with our age derivations of the other clusters.

3 PHASE SPACE CLASSIFICATION FOR THE GCS

In addition to the age and metallicity data discussed above, which trace a cluster’s internal properties, it is also useful

¹ http://www.astro.ufl.edu/~ata/public_hstgc/databases.html

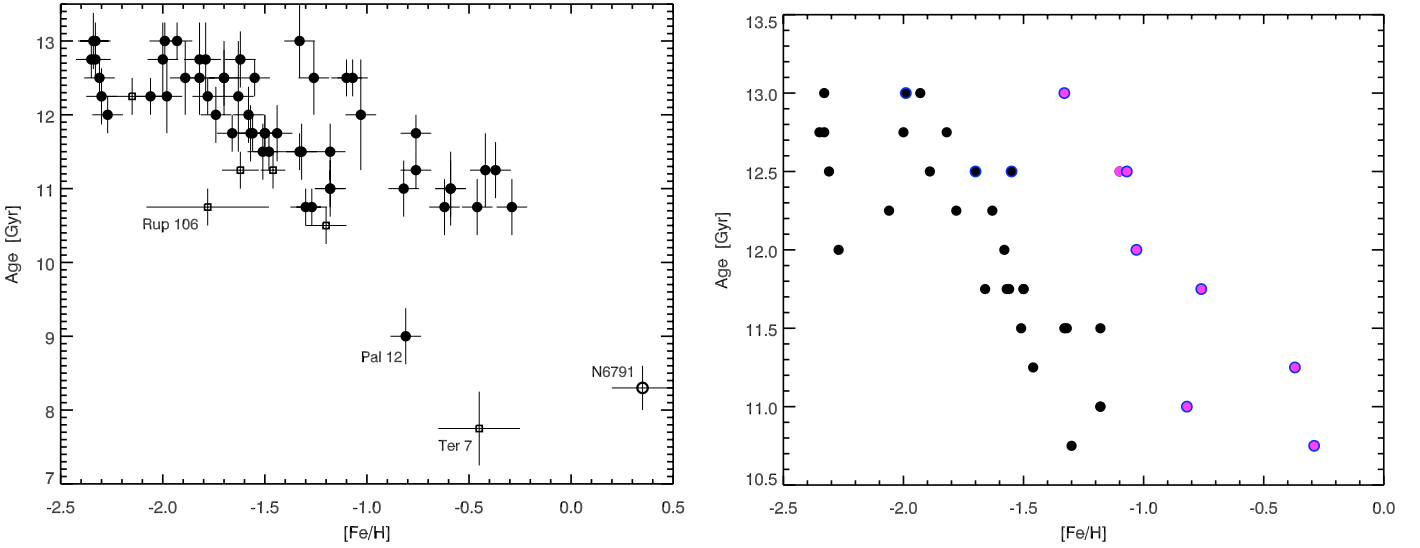


Figure 2. (Left panel) Age versus metallicity for the Milky Way GCs from VandenBerg et al. (2013) shown as the black filled circles. Six additional outer halo GCs presented in this work are shown as the open squares, and the metal rich cluster NGC 6791 from Brogaard et al. (2012) is plotted as the open circle. The bifurcation of the AMR into two “arms” is notable even down to the youngest ages. The right panel shows the AMR only for GCs which have phase space information. The points are colour coded by their probability of belonging to the disk or halo as described in the text. Blue circles indicate clusters which are more likely associated with the MW disk, pink filled points the disk clusters determined by eye simply by virtue of their metal rich offset in the AMR. Notably, the disk clusters span the full range of ages, but occupy the more metal-rich arm of the two distinct AMR sequences.

to consider GCs in the context of their host environment, in this case the MW. We therefore use GC phase space data from the compilation maintained by D. Casetti (and references provided therein; e.g., Casetti-Dinescu et al. 2007)² to classify globular clusters as either disk or halo populations using the probabilistic classification scheme described below.

For each GC i we can estimate the probability that it is associated with either the MW disk or halo as:

$$p(D, H|x_i v_i) \propto P(x_i, v_i|D, H)P(D, H) \quad (1)$$

where $P(x_i, v_i|D, H)$ is the likelihood of observing the phase-space coordinates x_i, v_i ($x_i \equiv X_i, Y_i, Z_i, v_i \equiv U_i, V_i, W_i$) given the (known) kinematics of a particular sub-component and $P(D, H)$ is the prior probability for GC_i to be associated with that component. In all cases we have assumed a uniform prior probability of membership. This analysis assumes that the kinematics of the MW GCs and field stars follow similar kinematic profiles - which holds in the general sense as far as differentiating halo- from disk-like orbits for old populations. Dynamical friction, while altering the orbits of accreted stars and GCs from dwarf galaxies, will not introduce strong systematic uncertainties in this classification as the GC stars are incorporated during cases of disruption, contributing to the observed halo velocity distribution.

We describe the stellar density profiles of the Milky Way thin disk, thick disk, and halo using equations (22)–(24) of Jurić et al. (2008), with the best-fitting parameters for the various scale lengths and density normalizations also taken from that work (their Table 10). We assume that the stellar

halo of the MW extends to 150 kpc (Deason et al. 2012), and following Pritzl, Venn & Irwin (2005), introduce a softening parameter $a = 20/\rho_0$ in order to keep the halo density finite in the inner regions. The velocity ellipsoids are taken to be Gaussian with the mean values and the dispersions for the thin disk, thick disk, and halo adopted from Table 3 of Venn et al. (2004) and references therein.

There is substantial evidence (see the review paper by Rix & Bovy 2013) suggesting that the MW thick disk is not a distinct component (i.e., separate from the thin disk), but rather represents a continuous extension of the thin disk. For example, Bovy et al. (2012b,a) showed that the structural (scale heights and lengths) and dynamical properties of “mono-abundance” populations in the MW disk smoothly change with chemical composition, therefore implying that the MW has a single disk with a continuum of properties. For this reason, we do not make a distinction between thin- and thick-disk systems, but simply classify them as members of the disk distribution in our calculations. Taking, $p_{disk} = p_{thin} + p_{thick}$, we assume the probability of a cluster belonging to either the MW disk or halo as:

$$\begin{aligned} \log(p_{disk}/p_{halo}) &\geq 0: && \text{(for the disk)} \\ &\leq 0: && \text{(for the halo)}. \end{aligned} \quad (2)$$

Moreover, we do not separate the halo populations as young (YH) or old (OH) as in the study by Mackey & van den Bergh (2005). The classifications in that work are based on the horizontal branch type as a function of metallicity, assuming that age is the main second parameter controlling the HB colour; however, the influence of possible helium enhancements on that metric complicates such divisions (see e.g., Gratton et al. 2010). Regardless, the halo clusters are canonically thought to have been accreted —

² <http://www.astro.yale.edu/dana/gc.html>

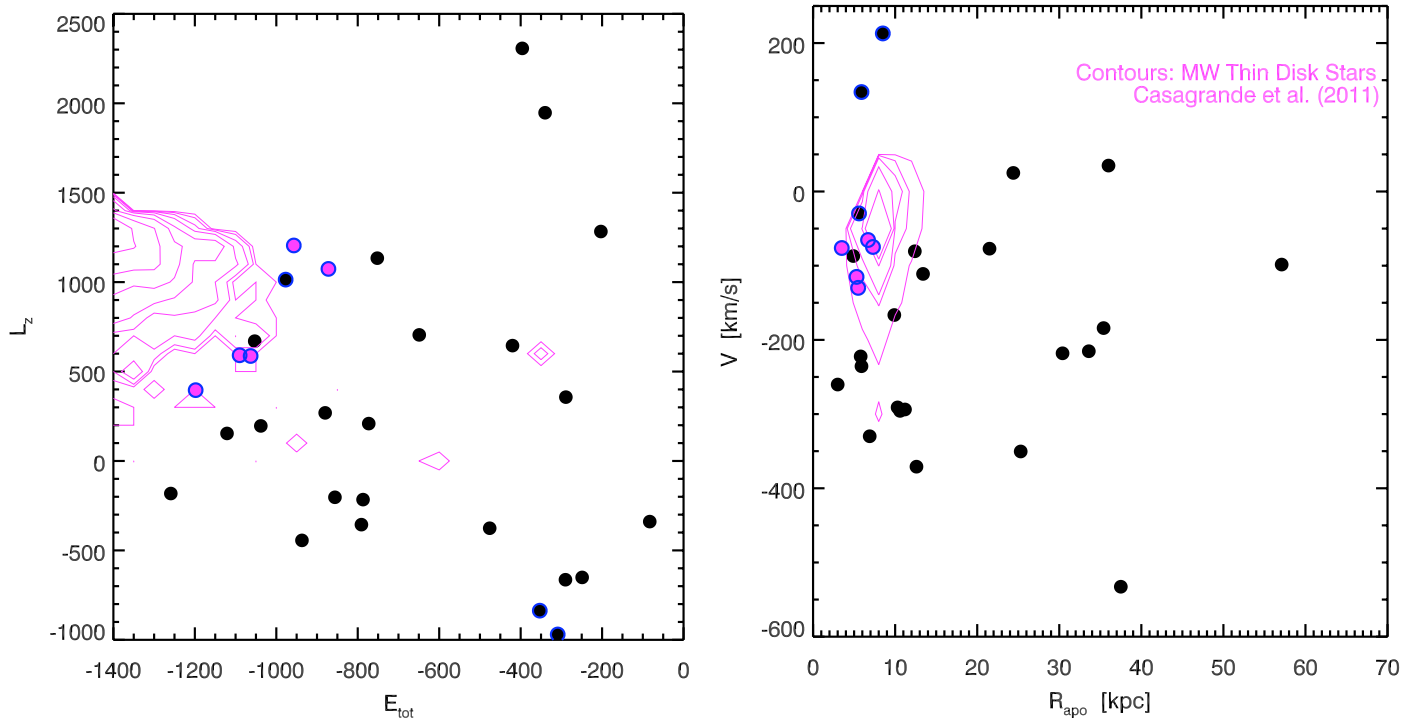


Figure 3. Common orbital properties for the clusters associated with the Milky Way disk (pink dots). The left panel plots the angular momentum versus total orbital energy, whereas the right panel plots the Galactocentric V velocity versus apocentric radius of their orbit. The disk GCs cluster together and also tend to overlap with the MW disk stars (pink contours) from Casagrande et al. (2011).

see, e.g., Mackey et al. (2013) for evidence in support of an accretion origin for 80% of the GC population in the outer halo of M31, as well as recent work by Keller, Mackey & Da Costa (2012), which reports similar findings for the YH clusters in the MW (see also Muratov & Gnedin 2010). Hence, for the present exercise, it is reasonable to treat all halo clusters as a single class.

4 THE SPLIT MILKY WAY GC AGE-METALLICITY RELATION

The upper panel of Figure 2 shows the AMR for all 61 Milky Way GCs in our sample. A split in the GC AMR is evident, with an offset metal-rich sequence running from approximately $[\text{Fe}/\text{H}] \sim -1.5$ and 13.0 Gyr down to $[\text{Fe}/\text{H}] \sim -0.4$ and 10.75 Gyr. The right panel plots as blue circles those clusters that have been identified as members of the disk from our Bayesian classification. The remaining black dots that populate the metal-poor branch of the AMR are associated with the halo. As the kinematic classification is dependent on the assumed density profile and velocity ellipsoids for the MW components, we also show with pink circles, those clusters that one would pick “by eye” as belonging to the offset AMR sequence. The kinematically classified disk clusters include all of those that one would select “by eye” as members of the offset sequence, giving us confidence that the classification scheme is appropriate.

Of the kinematically classified disk clusters which lay on the metal-poor branch of the AMR (blue circles around black dots), all have been listed in literature studies as be-

ing halo clusters from high mass progenitors, and are noted to have orbits which have likely been strongly affected by dynamical friction. In fact Dinescu, Girard & van Altena (1999) and Casetti-Dinescu et al. (2013) explicitly list NGC 6656, 6752, 6397, and 6254 as clusters which are likely halo members but whose orbits have been made more disk-like through orbital decay. The sole cluster in the disk sequence which is classified as a halo member is NGC 6723 (confirming the conclusions of Dinescu et al. 2003), although interestingly this cluster has kinematics and a location that confine it to the MW bulge. In conclusion, the most secure phase space classifications are completely consistent with a simple division of the AMR into two branches “by eye”.

It is somewhat reassuring that Pal 12 and Terzan 7 lie on the extension of the Halo AMR given that these clusters are thought to be associated with the accreted Sagittarius dSph. Law & Majewski (2010) identify M54, Terzan 8 and Arp 2 as GCs with a high probability of association with Sagittarius, while NGC 5053, Pal 12 and Terzan 7 are moderately likely to be associated. However the present MW AMR unfortunately offers little in the way of constraints on their membership, as halo GCs which are certainly not associated with Sagittarius also overlap with them in this parameter space. Therefore such membership studies will still be best probed through simulations of the tidal disruption of Sagittarius.

Figure 3 plots the total orbital energy and Z -component of the orbital angular momentum, along with the Galactocentric velocity (V) and orbital apocentric distance (R_{apo}) of the clusters. The disk clusters not only show common or-

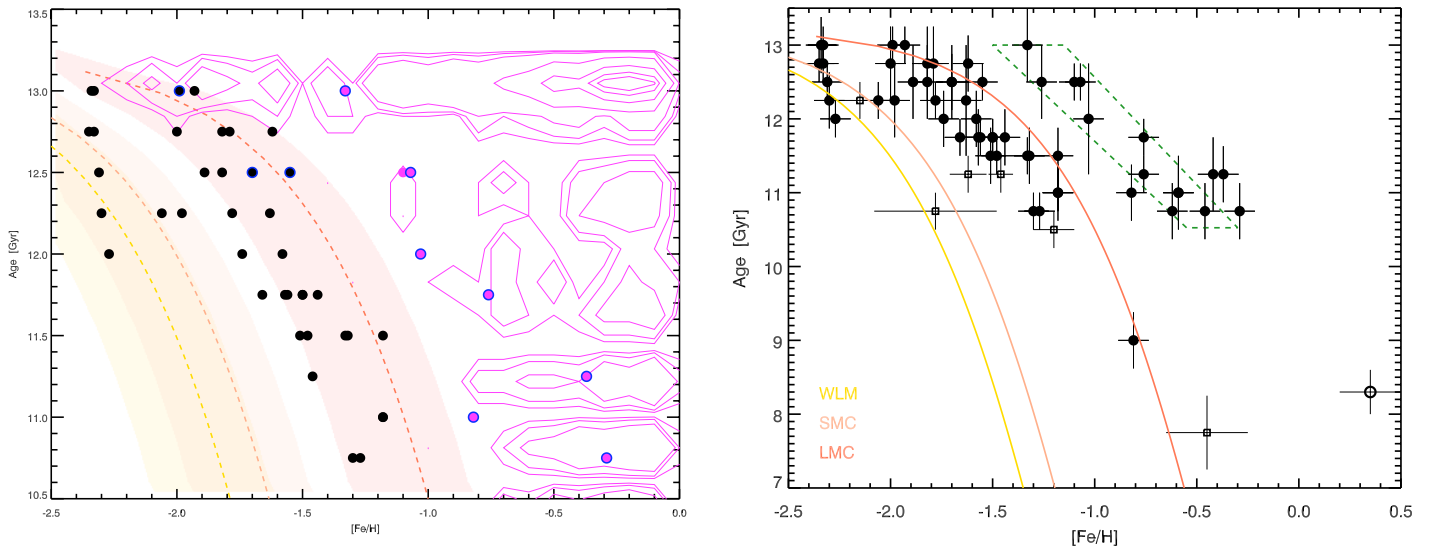


Figure 4. AMR of the MW GCs divided into the halo clusters and disk clusters, as determined from their orbital and phase space characteristics. Overlaid as the pink contours is the AMR from MW thin disk stars (Casagrande et al. 2011) which show good agreement with the disk GCs. The AMRs for dwarf galaxies of $M_* \sim 10^{7-9}$ from Leaman et al. (2013) and references therein are also overlaid, and the close agreement with the halo GCs suggest that they likely formed from dwarf galaxies of such masses and were accreted during the formation of the MW halo. Right panel shows the full range of age and metallicities, with the six new halo clusters shown as black squares, as well as a predictions for the AMR of the MW bulge GCs shown as the dashed green region (see §7.3).

bital properties, but also overlap with the data for MW thin disk stars (the density contours which are shown as magenta lines): the latter were derived from the updated analysis (Casagrande et al. 2011) of the Geneva-Copenhagen Survey (Nordström et al. 2004).

Having identified those clusters which are most likely associated with the disk of the MW, an obvious interpretation of the metal-rich arm of the split AMR is that it contains GCs that formed in-situ in the disk. It should be noted that the disk clusters are not simply the most metal-rich clusters, but the most metal-rich ones at any given age — and that they span the full range of ages encompassed by the halo clusters. The slopes of the AMR sequences are steep enough that it is not possible to make a simple cut at constant $[\text{Fe}/\text{H}] \gtrsim -1.5$ and have a “clean” sample of disk clusters.

If we assume that GCs metallicities trace the metallicities of their hosts when the bulk of stars formed, then a plausible interpretation of the offset between the metal-rich disk and the metal-poor halo AMRs follows from consideration of the galactic mass-metallicity relation (MMR). The offset in the GC AMR is approximately 0.6 dex in metallicity, which, given the slope of the MMR³ (Tremonti et al. 2004; Gallazzi et al. 2005; Lee et al. 2006; Kirby et al. 2011), translates into a difference in stellar mass of approximately $\Delta \log M_* \sim 2$ dex. Since the MW disk has a mass of $\sim (3 \pm 1) \times 10^{10} M_\odot$ (Robin et al. (2003); McMillan (2011)), this implies that the halo GCs are described by an AMR that is representative of

³ We note that the slope and differential shape of both the gaseous and stellar MMR in the mass range of interest are nearly identical (Lee, Bell & Somerville 2008; Kirby et al. 2011)

a galaxy with a stellar mass of a few $\times 10^{7-8} M_\odot$.⁴ This suggests that the halo GCs would have formed in dwarf galaxies comparable to the SMC, WLM, or even the LMC and Sagittarius.

This is empirically illustrated in Figure 4, where the AMRs for the MW thin disk, as well as those that have been derived for three dwarf galaxies are overlaid⁵ on the GC AMRs. The dwarf galaxy AMRs, which come from spectroscopic measurements of individual RGB stars, were compiled and presented by Leaman et al. (2013) and the data originally analyzed in the studies of Cole et al. (2005); Pompéia et al. (2008); Carrera et al. (2008a,b); Leaman et al. (2009); Parisi et al. (2010); Leaman et al. (2012).

The disk clusters tend to coincide with the metal poor edge of the MW thin disk AMR. This is likely because of the well known impact of radial migration (Sellwood & Binney 2002; Roškar et al. 2008) in scattering the disk AMR to higher metallicities at a given age — as well as the fact that we are considering clusters from the entire disk and some may be more closely linked to a metal poor “thick” disk component than the pure thin disk AMR. In addition the (Casagrande et al. 2011) ages were derived using stellar

⁴ We note that the *relative difference* in specific SFR (Karim et al. 2011) and metallicity (Zahid et al. 2013) between two galaxies of different mass stays roughly constant with time (back to redshift 3) as they evolve — at least for masses similar to the MW and the LMC.

⁵ We do not show the Sagittarius AMR due to the extreme difficulty in selecting clean, representative samples of RGB stars in this object, however the AMR given by Law & Majewski (2010) follows a similar shape and lies between that of the LMC and SMC.

evolutionary models without diffusion, though this effect is likely below the level of the previous two systematics.

Importantly, as the disk AMR from Casagrande et al. (2011) consists of primarily bright solar neighbourhood stars, it may provide only a partial view of the total disk AMR if the MW disk exhibits a strong metallicity gradient. A Complicating factor is that radial migration also shifts the observed AMR away from the “true” disk AMR. The interplay between these two systematics on the observed AMR is nearly impossible to quantify given the unknown evolution of the MW metallicity gradient, and when coupled with the 1 – 3 Gyr errors on the disk star ages, highlights the fact that we simply do not have an unbiased MW disk AMR with which to compare the disk GC’s AMR. Nevertheless the disk GCs are clearly separated and distinct from the halo GCs and even the most massive dwarf galaxy AMRs.

In this context where the age and metallicity of a cluster are intimately linked to the mass of its birth galaxy, NGC 6791 does not appear so unusual. This cluster has been extensively studied due to the apparent contradiction of having an old age, but high metallicity (for an open cluster), or an age much younger than is characteristic of metal-rich GCs. However it is clear from Figure 4 that it follows an extension of the AMR for the MW disk (or bulge; see §7.3), and in that regard may be completely consistent with expectations for clusters born out of a high mass progenitor environment.

In summary, the disk clusters exhibit an excellent empirical agreement with the AMR of the most metal poor MW disk stars from the Geneva Copenhagen Survey; while the AMR of the halo GCs spans the range shown by the three dwarf galaxies.

5 ESTIMATING THE ACCRETION HISTORY OF THE MILKY WAY FROM ITS GC SYSTEM

The halo clusters that form the metal-poor branch of the MW GC AMR are well fit by the AMRs of several Local Group dwarfs. However, this does not provide any explicit information on the relative number of those systems that may have been accreted by the MW. Several studies have attempted to place constraints on the number of accreted clusters (and their percentage of the halo mass), often using the variation of the structural or HB properties of the clusters with their position in the Galaxy to infer which ones may have been accreted (e.g., Mackey & van den Bergh 2005; Forbes & Bridges 2010)

Having the luxury of the split AMR and orbital data that enable us to classify the GCs into in-situ disk and halo systems, we may study this question further given the explicit link between the halo clusters and the mass(es) of their progenitor host (dwarf) galaxies. In Figure 4 there are $\sim 4 - 6$ clusters which are consistent with originating from a low mass WLM sized dwarf, while a great number more ($\sim 25 - 30$) are associated with a higher mass LMC-like progenitor. Is this consistent with expectations for the merger history of the MW — and with the expected number of GCs which might be accreted during the merger of dwarf galaxies with our Galaxy?

Answering this question requires comparing the ob-

served number of halo clusters from the split AMR and the total stellar mass of the MW stellar halo ($\sim 1 \pm 0.4 \times 10^9 M_\odot$; Morrison 1993; Bell et al. 2008; Deason, Belokurov & Evans 2011) to simulations of the merging history of the MW to check whether the GC population and stellar mass of the MW halo could have been accreted self-consistently. The new observational constraints from the mass-dependent splitting of the AMR in Figure 4 provide a first step in understanding how many dwarfs of a given mass merged to build up the stellar halo and the GC population of the MW.

To do this requires an estimate of the number of dwarfs of a given mass which merged with a MW-sized halo, as well as an expectation for the GC specific frequency S_N ⁶ for the dwarfs that were accreted. The differential number of subhalos of dark matter mass m that a larger galaxy of mass M accretes has been shown to be robust function of the total mass of the primary galaxy and its redshift, as given explicitly by Giocoli, Pieri & Tormen (2008) as:

$$N_{merged}(m) = A \int m^{-1.8} dm \quad (3)$$

The normalizing constant assumes that 25% of the stellar mass of the primary galaxy is accreted from smaller galaxies that have a mass fraction between $10^{-5} \leq \frac{m}{M} \leq 10^{-2}$. This gives the total number of merged subhalos as a function of their dark matter mass. We also explore an alternative formulation of the subhalo mass function from the high resolution n -body Aquarius Simulation of MW-sized halos; specifically, equation (7) of Boylan-Kolchin et al. (2010).

To associate a stellar mass m_* with every subhalo of dark matter mass m , we use the stellar-to-halo mass relation (SHMR) from Leauthaud et al. (2012), which has been robustly computed from an analysis of the observed weak lensing and spatial correlations in galaxy populations: this provides a measure of the stellar mass of a galaxy with a given dark matter halo. As in other works (Guo et al. 2010) the SHMR in the linear low mass regime is extrapolated for masses below $M_* \leq 10^8$. Together with equation (3) above, it is possible to compute the number of dwarfs of a given stellar mass which merge with the MW (assuming that its total dynamical mass is $\sim 8 \times 10^{11} M_\odot$; Vera-Ciro et al. 2013). This procedure thus enables us to track the buildup of the stellar halo.

The crucial question of how many GCs are contributed by an accreted dwarf requires an assumption about the specific frequency of GCs for each dwarf. Values of S_N typically range between 0.5 and 10, with some outliers, as in the case of M87 and Fornax which have S_N values approaching 20 (Mateo 1998; Peng et al. 2008). There is also evidence that S_N itself varies systematically with the luminosity or mass of a galaxy (i.e., Peng et al. 2008) - which may be linked to the galaxy SHMR (see also, Spitler & Forbes 2009). It is necessary to examine the implications of assuming different values for the specific frequencies, as we have no *a priori* knowledge of what the values of S_N were for the dwarfs that were accreted by the MW.

To estimate how many GCs will be accreted into the MW along with their host dwarf galaxies, we compute the

⁶ Defined as the total number of GCs hosted by a galaxy, normalized to its luminosity: $S_N = N_{GC} 10^{0.4(M_V + 15)}$

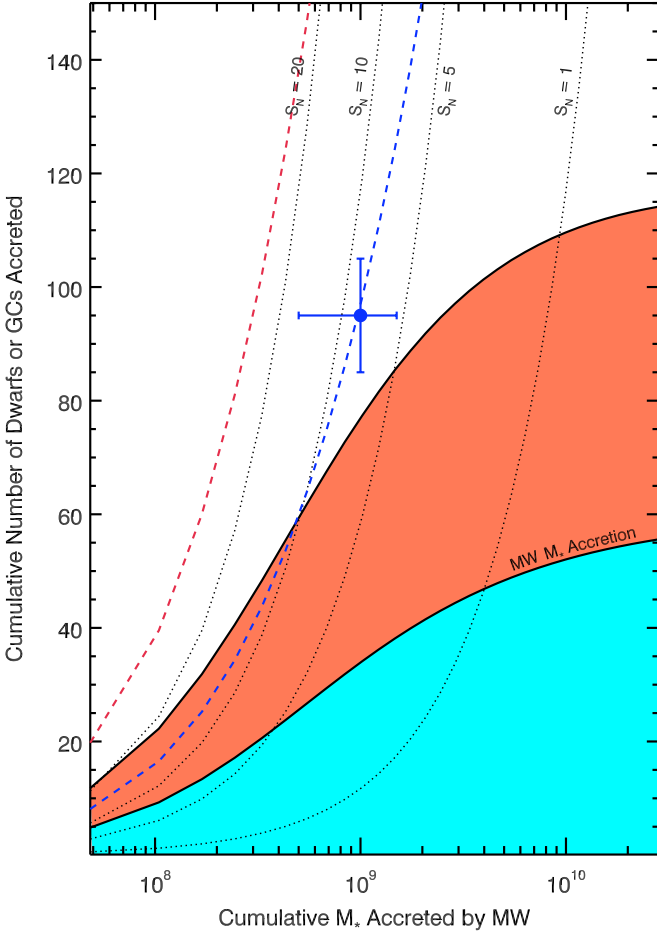


Figure 5. Cumulative stellar mass accreted by the Milky Way in assembly of its stellar halo, plotted versus the cumulative number of subhalos (dwarf galaxies) or GCs merged. Two subhalo mass functions are shown, one from Giocoli, Pieri & Tormen (2008) (solid black line bounding blue region), and one based on the merger history of the MW-sized halos in the Aquarius Simulations (Boylan-Kolchin et al. 2010) (black line bounding orange region). These solid lines show the cumulative number of accreted dwarfs by the MW. For various specific frequencies of GCs (dotted black lines), it is possible to show the cumulative number of GCs that were accreted in the same process. Observed number of halo GCs in the MW and stellar halo mass for the MW is shown as the blue point. While a fixed average $S_N \sim 7$ for all the merging dwarfs is possible, the dashed blue line shows that adopting a S_N which varies with mass as seen in observations of galaxies by Peng et al. (2008), reproduces the MW system without any fine tuning. Red dashed line shows the same Peng et al. (2008) S_N relation, but assuming the merger history of the Aquarius Simulations.

expected number of accreted dwarfs of stellar mass m_* as given by equation (3) and the SHMR, and multiply the result of that calculation by the number of GCs belonging to each dwarf of a given mass (which depends on a choice for S_N). The cumulative total of this product provides estimates of both the amount of stellar mass and the number of GCs that are contributed by accreting dwarf galaxies to the MW stellar halo. We repeat this for various fixed values of S_N as well as the mass dependent form of S_N from Peng et al. (2008) which is extrapolated to lower masses using

the SHMR of Leauthaud et al. (2012), as has been similarly done in Spitler & Forbes (2009).

Figure 5 plots the *cumulative* stellar mass accreted by the MW on the x-axis, versus the number of merged subhalos or GCs on the y-axis. The solid black lines show the cumulative mass growth of the MW stellar halo as the number of mergers increases for the subhalo mass functions of equation (3) and the relations in Boylan-Kolchin et al. (2010). The dotted lines indicate, for different specific frequencies, how many GCs are accreted by the MW as its stellar halo is assembled.

The blue dot indicates the observed values of the MW stellar halo mass, and the number of halo GCs. We have assumed that the ratio of disk to halo GCs seen in our sample ($N_{disk}/N_{halo} \sim 20\text{--}30\%$) is representative of the total GC population of the MW. On the assumption that the Galaxy has a total of $N_{tot} = 150$ GCs, of which 20 conceivably belong to the bulge, we obtain $N_{GC} = 95 - 105$ (the blue cross value) for our estimate of the current number of halo clusters.

At the observed stellar halo mass of $\sim 10^9 M_\odot$, Figure 5 indicates that the MW may have accreted $\sim 25 - 35$ dwarf galaxies (as indicated by the intersection of a vertical line at this mass with the relevant solid black curve). The Aquarius simulations predict a similar form for the growth of the mass that is accreted by the MW, but suggest that ~ 2 times as many dwarfs were merged in order to add a corresponding amount of mass. These dwarfs could easily contribute enough GCs to account for the entire population of the MW halo GCs, if they had, on average, a specific GC frequency $S_N \sim 7$. The dashed lines indicate how many GCs would be produced as a function of the accreted stellar mass if we used the mass dependent S_N scalings from Peng et al. (2008) for each of the two subhalo mass functions. The blue line shows excellent agreement with the MW values while the red line, which assumes the relations from the Aquarius Simulation, would be consistent with lower values for the MW stellar halo mass (or higher total numbers of halo GCs). This could easily be the case if some fraction of the MW's stellar halo was formed in situ, and/or additional outer halo GCs are discovered.

This self-consistent check on the accretion history of the MW is jointly constrained by the number of observed GCs in the halo, and its stellar mass. To first order this approach seems to offer useful constraints, nevertheless there are some obvious caveats; e.g., what fraction of stellar mass is fully accreted, and how many GCs survive? However we note that the observational constraints and relative fraction of accreted stellar mass are in good agreement with the recent results of Cooper et al. (2013) which tracked the assembly of stellar mass in high resolution n-body and semi-analytic simulations. In particular that work showed that MW sized galaxies could accrete 1 – 50% of their total (including disk and halo) stellar mass, and this was enough to *fully* assemble the stellar halo of the MW through mergers.

6 BIRTH ENVIRONMENTS OF THE ACCRETED HALO GCs

To help identify which galaxies could be responsible for the majority of the accreted GCs (instead of just the cumulative

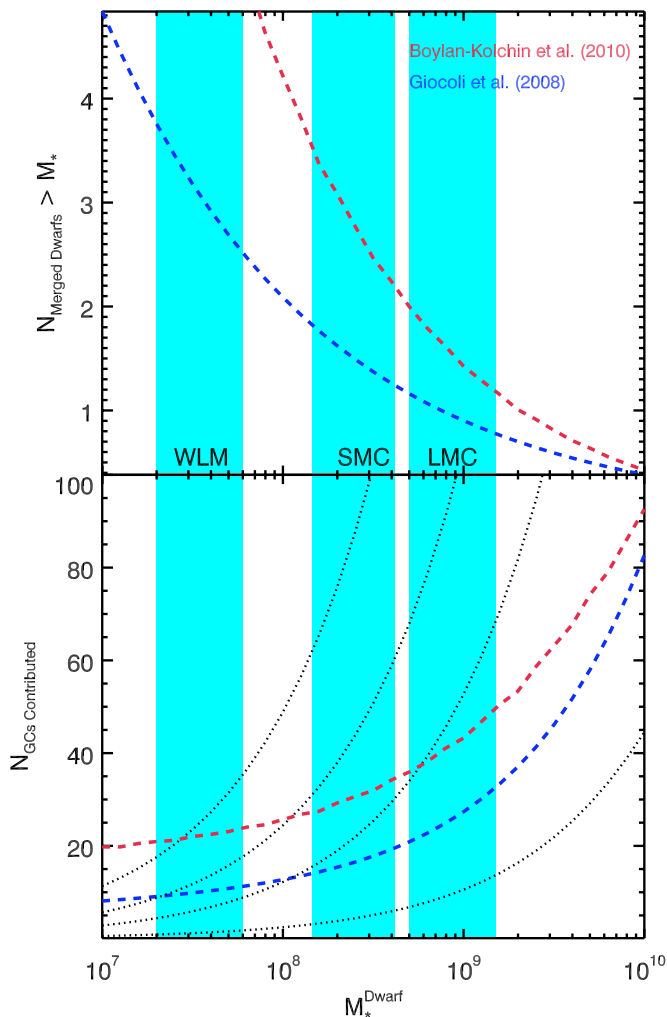


Figure 6. Top panel plots the number of accreted dwarfs of a given stellar mass expected to contribute to the MW halo over its buildup. Bottom panel plots, for various specific frequencies of $S_N = 20, 10, 5, 1$ (dotted black lines), what would be the total number of accreted GCs from dwarfs of that mass. The blue and red dashed lines show the mass-dependent S_N relation from the previous figure. Blue bands show for reference where the Local Group dwarf galaxies would fall on these relations given their observed stellar masses (McConnachie 2012).

number), Figure 6 plots the number of merged dwarfs as a function of the stellar mass of the dwarf, along with the total number of GCs which would be contributed by dwarfs of that mass. As in the previous figure, the number of GCs contributed by objects of a given stellar mass is defined as $N_{GCs,contributed}(m_*) = N_{GCs}(m_*) \times N_{merged}(m_*)$, where m_* is the stellar mass of the dwarf. The same curves of various specific frequencies (20, 10, 5, 1, and the Peng et al. (2008) S_N relation for the two subhalo distributions) are overlaid and we indicate where the three dwarf galaxies that were considered in the AMR plots in the previous section would fall on these curves.

These predictions are based on the assumed merger history from the simulations we consider, but suggest that if the MW has experienced 3 WLM-sized mergers, they would have contributed only a total of ~ 4 GCs, while one merger

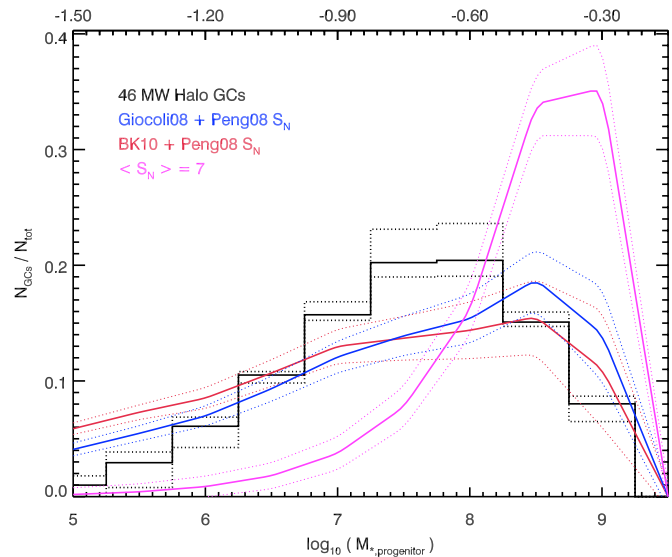


Figure 7. Progenitor mass of the dwarf galaxies from which the observed MW halo GCs could have formed, assuming the host galaxies offset AMRs translate directly into a mass decrement with respect to the MW disk. Top axis shows the numerical value of the AMR offset based on the slope of the MMR. Black histogram shows the result of applying this analysis to the 43 GCs classified as belonging to the MW halo. Red and blue dashed lines show the expected GC contribution as a function of progenitor mass using the two subhalo mass functions in the previous figures, and magenta line using a fixed S_N .

of an LMC-sized system would have contributed ~ 35 GCs⁷. This is in close agreement with positions of the halo GCs with respect to the AMRs of the LMC and WLM in Figure 4. Therefore it is plausible that most of the Halo GC system came from $\sim 6 - 7$ mergers of WLM- to LMC-sized dwarfs. It is interesting to note that, while the absolute number of merged dwarfs is different for the Giocoli, Pieri & Tormen (2008) or Boylan-Kolchin et al. (2010) subhalo mass distributions, they both suggest that the GC systems were primarily built from the 6-7 most massive mergers. We also note the good agreement with the early estimates from Unavane, Wyse & Gilmore (1996), and again the simulations of Cooper et al. (2010) who found that MW sized galaxies could accrete 20 – 80% of their stellar halo mass from the most massive progenitor dwarf galaxy in the mass range of $10^7 - 10^{8.5}$.

6.1 Implied Masses of GC Progenitor Galaxies from the Mass-Metallicity Relation and Offset AMR

A more direct comparison of the progenitor galaxy masses of the MW halo GCs with these model predictions, is possible by again leveraging the mass-metallicity relation in conjunction with the observed AMR. We begin by modelling the metal-rich branch of the AMR (that associated with

⁷ While the LMC itself does not contain this many *old* GCs, dwarfs of similar mass in Peng et al. (2008) show a wide range of S_N values.

the in-situ disk clusters) as a linear fit between the points $([\text{Fe}/\text{H}], \text{Age}) = (-1.5, 13.0)$ and $(-0.5, 10.75)$. From the near constant offset in metallicity at all ages for the disk GCs (and similar shape of the observed dwarf galaxy AMRs), we can, to first order, assume that the slope of all of the AMRs in this early epoch is invariant. Any dwarf galaxy will then have an AMR that is simply offset in metallicity from the disk AMR, by an amount which depends on the total stellar mass of the dwarf.

For each halo GC, (the black dots in Figure 2), we compute its metallicity offset from the disk AMR, $\Delta[\text{Fe}/\text{H}]$. With the observed slope of the mass-metallicity relation from Kirby et al. (2011), the value of $\Delta[\text{Fe}/\text{H}]$ for each GC is transformed into a mass decrement from the MW disk, thereby giving a coarse estimate of the mass of the progenitor galaxy in which that GC might have formed. This is obviously most useful in a differential sense, as the exact shape of the AMR and disk mass as the MW evolves is not precisely known.

Figure 7 displays the result of this analysis, wherein we show the average distribution of implied progenitor dwarf galaxy masses for all 46 MW halo GCs. This is essentially a convolution of the subhalo mass function with the number of GCs per dwarf galaxy of a given mass. The black histogram represents the average distribution found from 50000 Monte Carlo trials of this process, in which the observational errors in age and metallicity for the GCs, as well as the errors on the fit to the disk GC AMR were simultaneously incorporated.

To directly compare these to the expected distribution from simulations of the MW accretion history, we compute Monte Carlo realizations as follows. For a given trial we randomly pick 50 dwarf galaxies to merge with the MW with their distribution in masses weighted according to the subhalo mass function of Equation 3 (or Equation 7 of Boylan-Kolchin et al. (2010)). We take a lower limit for the progenitor galaxy mass as $M_* = 10^5$, as that is a mass close to those of most GCs themselves, and the maximum progenitor galaxy mass as $M_* = 10^9$, as we should not expect mergers greater than the total MW stellar halo mass. The number of GCs per progenitor galaxy is computed for each of the 50 dwarfs assuming either the Peng et al. (2008) S_N , or a fixed $\langle S_N \rangle = 7$, producing a predicted distribution of the number of accreted GCs as a function of the mass of their progenitor galaxy. This is repeated for 5000 trials, and the mean and standard deviation of the distributions recorded — which we show as the coloured curves in Figure 7.

There is good agreement between the black histogram, which shows the estimated progenitor masses implied by the offset AMRs, and these expectations from n-body simulations of the MW's assembly. Dwarfs with masses $\leq 10^6 M_\odot$ contribute only a few percent of the total MW halo GCs, with the contribution increasing until a maximum contribution is reached, from dwarfs of $\sim 10^{8.5} M_\odot$. Notably, the predicted distribution when assuming a constant S_N for all dwarf galaxies results in far too many GCs from high mass progenitors. This would suggest that there needs to be at least some variation in the S_N values of the accreted system — therefore the mass dependent variation of S_N observed

in the Virgo cluster sample of Peng et al. (2008) may be representative of many systems⁸.

The distribution of implied progenitor masses shown by the black histogram allows us to study how many significant progenitor dwarfs built up the total stellar halo and GC system following the definition in Cooper et al. (2013)

$$N_{sig} = \frac{(\Sigma m_{*,progenitor})^2}{\Sigma m_{*,progenitor}^2}. \quad (4)$$

We find a value of $N_{sig} = 11$, in good agreement with that work which showed that MW sized stellar halos can be built up by ~ 10 significant progenitors in some cases. Importantly, our semi-empirical estimate of N_{sig} is completely independent of an assumed subhalo mass function, as the progenitor masses are calculated solely from the offset AMR, and provides a unique comparison to such simulations. We note however that the exact distribution of the progenitor masses is somewhat sensitive to the relative shape of the MW and dwarf galaxy AMRs. Assuming no pre-enrichment in the MW disk AMR would lead to a suppression of the lowest mass progenitors in the histogram, but would still not produce a peak at the very highest masses.

6.2 Correlations between the Properties of GCs and their Implied Progenitor Galaxies

To further illuminate the link between the MW GC system and the host galaxies of accreted halo GCs, Figure 8 plots the implied progenitor galaxy masses versus several structural and orbital properties of the globular clusters. The disk GCs are shown as the magenta points and in this exercise are placed at a progenitor mass close to that of the MW disk. Linear least squares fits are shown as dotted lines, and in all cases are computed based solely on the halo clusters.

One noticeable trend is that the mass of a GC and its central density (traced by V_{esc} and σ_0) are correlated with the mass of the galaxy in which the GC was born. While speculative, these correlations may provide an explanation as to why GCs with the highest V_{esc} and σ_0 in V13 tended to show the strongest evidence for helium abundance enhancements (as inferred from the relatively steep slopes of their subgiant branches in the observed CMDs). This result is particularly puzzling, as the *present-day* cluster masses should not be predictive of past masses and their capability, or not, to retain the ejecta from a primordial stellar generation and to produce second-generation stars with significant He abundance variations. Figure 8 suggests that the most massive, densest clusters may form predominantly in the highest mass dwarf galaxies (although a range in V_{esc} and σ_0 is apparent at any progenitor mass, suggesting perhaps that even within a single dwarf, GCs and molecular cloud mass may have a dependence on local environment; e.g., Meidt et al. 2013).

Therefore, when they are accreted by the MW, those

⁸ We note also that the differential distribution of progenitor masses we recover using the Spitler & Forbes (2009) relations is nearly identical to what we find using the Peng et al. (2008) formalism. However as the former relation requires an assumption on the mass of individual GCs it provides little leverage on the total number of GCs accreted (i.e. Figure 5 and 6).

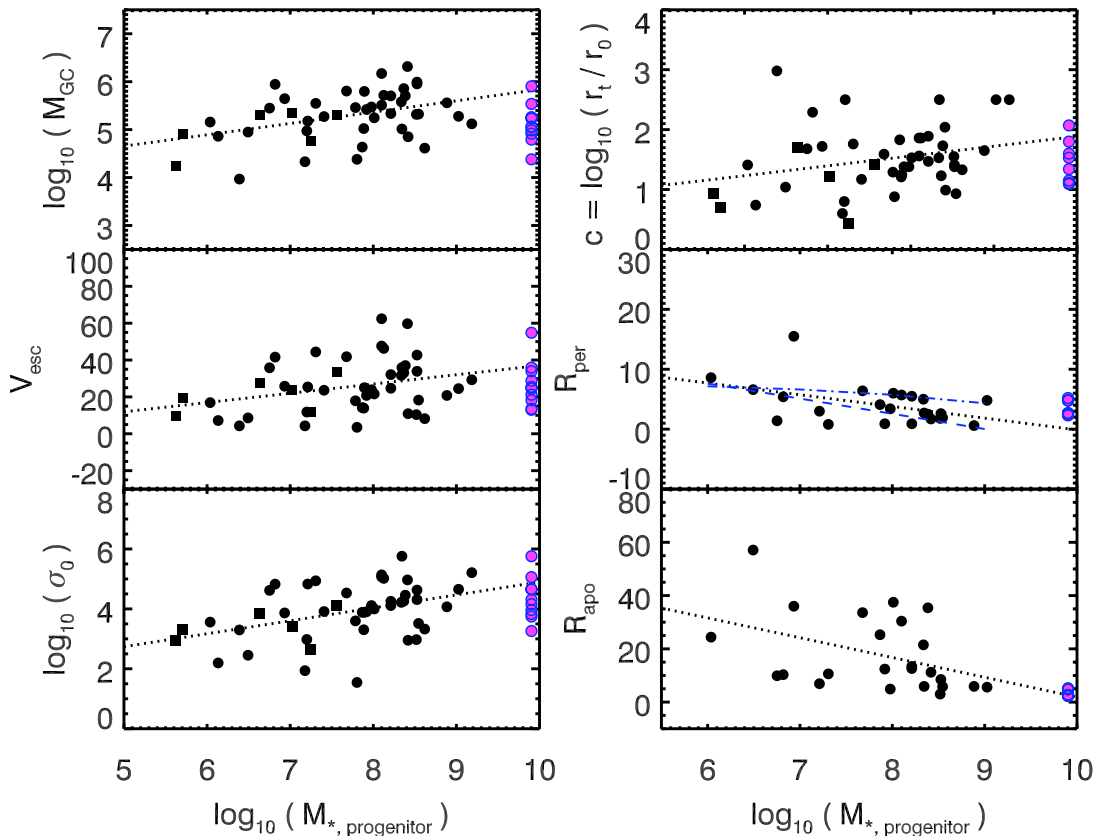


Figure 8. Structural and orbital properties of the MW halo GCs as a function of the mass of their progenitor dwarf galaxies. Magenta points represent the MW disk GCs. Dotted lines are linear least squares fits to solely the halo GCs. Blue dashed lines show predicted orbital decay as a function of dwarf galaxy mass due to dynamical friction (see text).

GCs would be embedded in a much larger dark matter and baryonic envelope which could mitigate the effects of tides and ram pressure, perhaps allowing them to retain ejecta from their first generation of stars.

The correlation between concentration parameter ($c = \log_{10}(r_t/r_0)$; Harris 2010) and progenitor mass in the top right panel of Figure 8 is particularly interesting in light of the correlation between GC size and colour (or metallicity) seen in the MW and many extragalactic GC systems in giant ellipticals (e.g., Larsen et al. 2001). As the correlation persists over many radii within individual galaxies, Larsen et al. (2001) suggested that this may reflect a primordial correlation which is setup in the birth of the GC. They suggested that perhaps the most compact GCs form in the largest gas clouds (which would be found in the largest galaxies) preferentially. This interpretation would seem to be supported by the trend in the top right panel of Figure 8, and would suggest that the correlation exhibited between concentration and colour or metallicity is a consequence of the lower mass progenitor systems in which preferentially low metallicity systems (of a given age) are found.

The bottom two right-hand panels of Figure 8 show that there is also a trend for GCs with the lowest host galaxy masses to be found at larger Galactocentric distances. This correlation may arise as a consequence of the orbital decay of a dwarf galaxy as it is accreted onto the MW. Galaxies with the highest masses (and the GCs they host) will prefer-

entially sink to the centre of the MW via dynamical friction. This effect is enhanced further when the mass growth of the MW is taken into account or for more eccentric orbits⁹. We note, however, that there is no strong evidence from simulations for systematic variations in the radius as a function of the progenitor mass (Wang et al. 2011).

An order of magnitude estimate for the varying impact of dynamical friction on dwarfs of different masses can be estimated from the analytic expressions given in Zhao (2004). These formulae for dynamical friction consider both tidal stripping of the accreted satellite, and growth of the MW halo over time, and the change in orbital radius with time is characterized by 2-parameter functions of the form:

$$\Delta r(t) \simeq \frac{2\pi G t_f}{(t_f - t_i) V_f} m_i \left[1 - \left(1 - \left(\frac{m_f}{m_i} \right)^{1/n} \right)^n \right] \int_{t_i}^{t_f} t^{n-p} dt \quad (5)$$

We compute this quantity for dwarfs of initial mass $m_i = 10^6, 10^7, 10^8, 10^9$, and track the dwarfs orbital decay from $t_i = 4$ Gyr to $t_f = 13$ Gyr where the remnant accreted dwarf mass is reduced to $m_f = 10^5$. We then compare the relative orbital decay for each of the different mass dwarfs,

⁹ However as shown by van den Bosch et al. (1999), there is no total evolution in orbital eccentricity, which likely explains why the slopes of the pericentric and apocentric radii relations are so similar.

allowing for comparison with the right hand panels of Figure 8.

A reasonable reproduction of the observational data is found for a mass loss parameter value of $n = 1.01$ (corresponding to a near linear case, suitable for isothermal dwarf galaxy models) and qualitatively reproduces the trend of radius versus dwarf galaxy progenitor mass seen in the right hand panels of Figure 8. We also show the formulation given in Cote, Marzke & West (1998) which has a milder slope due to the fact that it doesn't incorporate mass loss for the host systems or growth of the MW.

A further correlation between the orbital properties of GCs of similar progenitor mass is shown in Figure 9. The cluster progenitor masses are computed for each cluster for 50000 Monte Carlo trials, with the errors on age, metallicity and disk AMR incorporated as described previously. For each trial the clusters are grouped by progenitor mass and the orbital properties of the clusters in each mass bin are recorded. The panels in Figure 9 show that *over many realizations* the GCs from different progenitor masses tend to show common and distinct orbital properties. The GCs from the highest mass clusters again show properties that are consistent with having been operated on by dynamical friction. The mild separation of clusters by their progenitor mass in Figure 9 provides some support that our simple estimates for progenitor mass are physically consistent with their phase space properties in this context. We stress however that there are relatively large, yet unquantified systematic errors associated with the derived orbital quantities used in this Figure. Similarly, the particular separations by progenitor mass in this Figure are not expected to be a generic prediction for all galaxies, as the variety in merger history is large; however more detailed orbital models of individual GCs in the MW or external galaxies could continue to explore such clustering of GCs in phase space in this way.

7 DISCUSSION

7.1 What Controls the Range in GC Ages in the MW

It is well known that the MW GC population shows a sharp truncation in their relative ages, with no GCs younger than ~ 8 Gyr (van den Bergh 2000). The in-situ disk clusters, and even the more metal-rich of the halo clusters (which would have come from the most massive accreted dwarf galaxies) have GCs that span the first 2 – 4 Gyr of the MW's history. The more metal poor GCs (corresponding to the lower mass WLM-sized dwarfs) do not contain similarly young clusters (note the deficit of points around -2.0 , and 11.25 Gyr in Figure 2)¹⁰.

Indeed WLM itself, with a stellar mass of $\sim 5 \times 10^7 M_{\odot}$, has only one old GC, while the LMC and SMC, and particularly Sagittarius are known to have extended cluster AMRs of 3 Gyrs or more (Glatt et al. 2008; Law & Majewski 2010;

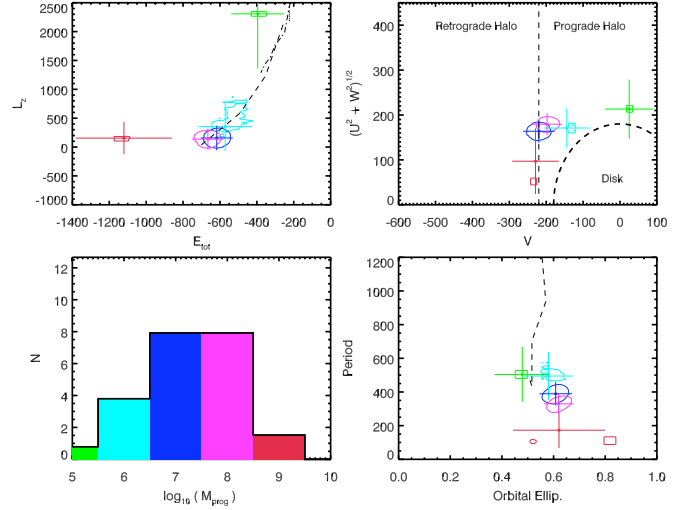


Figure 9. Monte Carlo simulations of orbital properties for MW halo GCs. Bottom left panel shows histogram of progenitor masses after 50000 trials where the cluster progenitor masses are computed taking into account errors on their age, metallicity and AMR of the MW disk. The histogram bins are colour coded by mass, and the other three panels show the 1σ contours, and median distribution values (*crosses*) of each mass bin for various orbital parameter spaces. There is a clear tendency for the GCs to separate by progenitor mass in their orbital properties. Lines in the top left and bottom right panels show expectations for the impact of dynamical friction from (van den Bosch et al. 1999).

Colucci et al. 2011). This could be an indication that less massive dwarfs, which exhaust their gas reservoirs quickly (perhaps due to the efficient SNe induced blowout of gas from their shallow potential wells), form GCs for only a short interval of time. Alternatively, it may be the case that their SF efficiencies are so low, or that they are more susceptible to reionization (e.g. Strader, Brodie & Forbes 2004) so that few stars (and GCs), are able to form before they are accreted.

A complementary picture could be that the lowest mass dwarfs, in which relatively few GCs formed due to reasons given above, were accreted earlier by the MW. This would effectively truncate their cluster AMR sooner than in the case of higher mass dwarfs which were accreted at later times by the MW, and therefore had time to form GCs over a longer epoch. This is supported by simulations of MW-sized halos, where the average accretion time of low-mass dwarfs is found to occur earlier by ~ 4 Gyr (Boylan-Kolchin et al. 2010). If massive GCs are necessarily formed in very intense starbursts (Elmegreen, Malhotra & Rhoads 2012) or massive GMC collisions (Furukawa et al. 2009), it could simply mean that these conditions are not found in dwarf galaxies or the MW (which shows a relatively quiescent SFH).

Such a scenario might also explain why the MW is devoid of GCs younger than ~ 8 Gyrs, with even the most metal-rich halo GCs having older ages. In order to have an increasingly longer GC formation epoch, a dwarf would require both a late time accretion to the MW and be a comparable fraction of the MW mass. As such high-mass mergers are increasingly unlikely in CDM cosmologies, the lack of GCs younger than ~ 8 Gyrs may simply be telling us

¹⁰ The notable exception is Ruprecht 106 at $[Fe/H] = -1.78$ and 10.75 Gyr in this plot, however as discussed in §2 the metallicity of this cluster is particularly uncertain, with Dotter, Sarajedini & Anderson (2011) favouring a value of $[Fe/H] = -1.5$.

that there has not been any accretion of dwarfs with stellar masses greater than $10^9 M_{\odot}$.

7.2 Formation Theories for the MW GC System in the Context of this AMR

The primary theories for the assembly of GC systems in large galaxies (see review by Brodie & Strader 2006) are: accretion of GCs in dwarf galaxies during hierarchical assembly (Cote, Marzke & West 1998), merging of large galaxies (Ashman & Zepf 1992), and in-situ formation (Forbes, Brodie & Grillmair 1997). Observational data for MW and extragalactic systems has revealed that most GC systems are comprised of a red and a blue population which are generally considered to reflect the underlying metallicities of the GCs (although see Yoon et al. 2011; Blakeslee et al. 2012). Correlations between the mean colour of the red, and blue GC populations with host galaxy mass have been used to help understand possible formation avenues.

This is intrinsically challenging given the relatively unknown age distribution of the blue GCs in extragalactic systems, which makes inferences concerning the formation time, duration and mechanism of in-situ or accreted GCs difficult. The analysis presented here suggests that an accretion formation for the metal poor (halo) GCs in the MW is supported by the details of the AMR shape with respect to the disk clusters. Much of our analysis is in line with the earlier proposals from Cote, Marzke & West (1998), and the primary tension of that work with observations — that the predicted red and blue populations of GCs show no mean age difference — is no longer inconsistent with this MW GC AMR. Similarly the work of Muratov & Gnedin (2010) which incorporated many aspects in agreement with our analysis, is not problematic in its suggestion that large age spreads are likely in both the metal poor (MP) and metal rich (MR) GC populations (with that study also finding a similar ratio of in-situ disk clusters as seen here). Additionally the observation that GC metallicities in dwarf galaxies are lower at all ages than in higher mass galaxies (Strader et al. 2005) is not a point of concern with accretion models, but is a natural expectation given the mass metallicity relation for the accreted (dwarf) galaxies.

Alternatively in-situ theories, which were envisioned to explain blue GC populations with a narrow range of old ages (Forbes, Brodie & Grillmair 1997; Beasley et al. 2002), typically find that the MP GCs should be older by ≥ 2 Gyr than the MR GCs and have a very narrow range of ages. In some cases the in-situ theory (e.g., Forbes, Brodie & Grillmair (1997)) produces a narrow range of ages for the MR component as well, as the dynamical time for the galaxy during its secondary collapse has decreased. To first order both aspects of these theories are ruled out for the MW, as the MR and MP AMR sequences have identical average ages, and age spreads.

Hybrid theories (Strader et al. 2005) may have less tension with the MR AMR but suggest that the blue GC population is not assembled via hierarchical accretion. This new AMR does not invalidate such theories in principle, however the suggested high redshift, rapid formation epoch for blue GCs is again problematic in light of the halo GC age range of the MW. The main argument in Strader, Brodie & Forbes (2004) against accretion of DGs to assemble the

blue GC population is that it would tend to erase the correlation between average blue GC colour and host galaxy luminosity. This may not necessarily be the case when one considers that the GCs are pre-enriched from dwarfs that themselves fall on the mass-metallicity relation for galaxies. Therefore the GC population of the dwarf galaxies reflects the self-enriched history of their birth environment (Leaman 2012), and a *hierarchical* accretion scenario (see e.g., Fig. 14 of Cooper et al. 2013) would also produce a correlation between the metallicity of the blue GC population and host galaxy metallicity.

Certainly in-situ or hybrid formation models which don't truncate the epoch of formation for blue GCs may be possible, however it could be difficult to produce two in-situ populations of GCs with the same age distributions but offset in metallicity within a single galaxy.

7.3 Prediction for the AMR of the MW Bulge Globular Clusters

V13 did not include any of the highly reddened clusters thought to be associated with the bulge of the MW in their sample. These clusters, in particular, provide a test of how the central bulge of the MW formed; i.e., via mergers or through secular evolution, and therefore their ages and metallicities can be used to probe these two scenarios. Our interpretation of Figure 4 indicates that the metallicity offset between the disk and halo branches of the AMR is driven by the relative mass of the self-enriching environment (Milky Way disk, or SMC sized dwarf galaxy) in which the clusters formed.

In this context, the MW bulge as a distinct environment with a unique chemical enrichment history (as compared with the disk), should have clusters that formed in-situ which follow an AMR that is proportional to the stellar mass of the bulge. Mass models from McMillan (2011) give the bulge stellar mass as $\sim 9 \times 10^9 M_{\odot}$ with earlier studies quoted in that paper favouring higher masses of $(2.4 \pm 0.6) \times 10^{10} M_{\odot}$. Given the stellar disk mass of $\sim (3 \pm 1) \times 10^{10} M_{\odot}$, the small offset in stellar mass between the two components would suggest that the bulge clusters of a given age have close to the same metallicities as disk clusters of the same age, or are nearly coeval with disk clusters at a given [Fe/H] value. This region is shown as the dashed green polygon in Figure 4

Using recently measured spectroscopic metallicities for bulge clusters from Saviane et al. (2012) and others in the Harris (2006) GC catalogue¹¹ we might predict the ages of some of the bulge GCs (under the assumption they formed in-situ). The bulge clusters near [Fe/H] $\simeq -1.35$ (including HP 1, AL 3, NGC 6522, NGC 6540, Terzan 4, and NGC 6325 as well as more metal poor clusters) are expected to have ages of ~ 12.75 Gyr. Similarly, it is our expectation that clusters with [Fe/H] ~ -1.05 (e.g., NGC 6558, Terzan 9), ~ -0.5 (NGC 6356, NGC 6441), and ~ -0.2 (NGC 6528, NGC 6553, NGC 6440) will have ages of approximately 12.0, 10.75, and 10.0 Gyr, respectively. Due to the difficulties in determining absolute cluster ages, the prediction most easily

¹¹ <http://physwww.mcmaster.ca/harris/mwgc.dat>

tested is that the ages of NGC 6558 and Terzan 9 are expected to be $\sim 1.5\text{--}2$ Gyr older than NGC 6528/6553/6440.

As shown by Cote, Marzke & West (1998), such analyses can also be applied to more distant galaxies (M31, or the GC systems of elliptical galaxies) in order to place constraints on the relative number of accreted GCs, and to achieve a better understanding of the formation environments of GCs.

7.4 Caveats

In this analysis we have assumed that the entire halo population of GCs and MW stars were formed through accretion. There is conflicting observational evidence in the literature as to whether the halo of the MW shows two distinct components (Beers et al. 2012; Schönrich, Asplund & Casagrande 2011), and if so, whether one of the components is incompatible with an accretion origin. Certainly there is theoretical work suggesting that some fraction of the MW halo stars may have formed in-situ from high-redshift accreted gas, and then been dynamically heated into the MW halo through later mergers (e.g., Zolotov et al. 2009). Such simulations have found that the in-situ fraction strongly depends on the merger history of the MW. Unfortunately it is not known whether any GCs would also form in-situ through the same process; therefore, we simply note that the assumed accreted stellar mass of the MW halo can be considered an upper limit. Any contribution by stars formed in-situ would then lower the number of merged dwarfs (and hence GCs) in Figure 5. Whether or not the observed GC fraction could be used to constrain the in-situ halo fraction in this way is likely not possible with this analysis however.

Similarly, higher-order chemical abundances (α -, r - and s -process element ratios) have the ability to discern whether the chemical evolution of the GCs and halo field stars are similar. Results are complicated by the unknown formation epoch and environment for GCs. However, there is evidence in the MW, LMC, and Fornax that the metal-poor GCs show similar $[\alpha/\text{Fe}]$ ratios as in the field stars that have similar $[\text{Fe}/\text{H}]$ values ((Pritzl, Venn & Irwin 2005; Hill 1997; Letarte et al. 2006; Mucciarelli et al. 2011), but see Mateluna et al. 2012). This helps to alleviate one concern with the present analysis, in that we do not consider what fraction of GCs may have evaporated during the accretion procedure. While there may have been many small GCs which were disrupted and dispersed through the halo during accretion, we can consider them part of the stellar mass contributed by dwarfs in light of the above results.

The same chemical similarity is not true of the MW halo stars and the field stars in the surviving dSph galaxies (Venn et al. 2004). However we note that this is not particularly constraining for the current problem as the dwarf galaxies studied are the *surviving* population of dSphs, which may have very different chemical properties from the ones that merged with the MW (c.f., Gilmore & Wyse 1998), especially if the mergers with the MW happened early, before significant chemical evolution of the dwarfs could have occurred. Certainly, if the lowest mass dwarfs were accreted first, the $[\alpha/\text{Fe}]$ ratios could well be markedly different from what is observed in dwarfs today. Additionally, Figure 4 suggests that high-mass dwarfs ($\sim 10^{8-9}M_{\odot}$) were the predominant contributors to the GC population of the MW halo (see also Cooper et al. 2013), in which case, the chemical abundance

differences between the MW field stars and low-mass dSphs ($\sim 10^{6-7}M_{\odot}$) is not necessarily a relevant constraint on this scenario.

Finally, a split AMR could generally be interpreted not only as an offset in metallicity at fixed age, but as an offset in age at fixed metallicity. The latter might be a signature of a two-phase galaxy collapse (e.g., Hartwick 2009). However given that this particular AMR split does not extend to the lowest metallicities and the range in ages are identical, the data analyzed here seem to favour the scenario presented in §4 over the interpretation of an age offset.

8 CONCLUSIONS

Our analysis of the AMR in the MW GC system has identified a clear split in the sequence, with approximately one-third of the clusters being offset by 0.6 dex in metallicity from the more populous metal-poor branch¹². The corresponding mass decrement as implied by the MMR, coupled with subhalo merging statistics from simulations of MW-sized halos, has led us to postulate that the MW halo GC system could have been assembled in a consistent manner simultaneously with the MW stellar halo. This interpretation was also suggested by Elmegreen, Malhotra & Rhoads (2012), who inferred from the space density of Ly α emitting galaxies that some metal-poor (halo) GCs formed in dwarfs with stellar masses comparable to WLM, in agreement with our independent analysis.

A notable implication of the new AMR is that the identical mean age, and spread in ages shown by the metal rich disk GCs and the metal poor halo GCs is difficult to reconcile with in-situ formation for the latter population. The ~ 4 Gyr age spread among the MW's metal poor halo GCs could imply that the blue GCs in extragalactic galaxies need not have formed in a truncated epoch due to reionization. Similarly correlations between the average metallicity of the blue GC population and the host galaxy mass is consistent with the hierarchical accretion origin of the halo GCs.

The observational result of the split AMR is only made possible by the robust age derivations from V13, which have revealed and corrected several systematics in past analysis of the MW GC ages. Past studies of the AMR of the MW GCs have therefore been limited by the data in reaching conclusions concerning the origin of various GC populations (e.g., Forbes & Bridges 2010).

Our interpretation of the bifurcated AMR as a diagnostic for understanding the birth environment for GCs, is also useful as a predictive tool for the MW bulge population, and may offer valuable constraints on simulations that investigate the amount of accreted stellar mass in the MW halo. Further high fidelity age and orbital properties for GC systems in the MW, M31, and other galaxies will continue to aid such ventures.

¹² The data for the AMR figures in this paper can be found in Table 1 of V13, and is also available upon request from the authors.

ACKNOWLEDGMENTS

The authors thank the anonymous referee for useful comments which greatly improved this manuscript. We thank Ata Sarajedini for informing us where to obtain the publicly available photometry for five of the outer-halo GCs for which we have determined ages. The authors also thank Kim Venn, Else Starkenburg, Alan McConnachie and David Hartwick for several helpful comments, which improved this paper. RL acknowledges financial support to the DAGAL network from the People Programme (Marie Curie Actions) of the European Unions Seventh Framework Programme FP7/2007-2013/ under REA grant agreement number PITN-GA-2011-289313, whereas the contribution of DAV was supported by a Discovery Grant from the Natural Sciences and Research Council of Canada.

REFERENCES

- Ashman K. M., Zepf S. E., 1992, *ApJ*, 384, 50
 Beasley M. A., Baugh C. M., Forbes D. A., Sharples R. M., Frenk C. S., 2002, *MNRAS*, 333, 383
 Beers T. C. et al., 2012, *ApJ*, 746, 34
 Bell E. F. et al., 2008, *ApJ*, 680, 295
 Bennett C. L. et al., 2012, *ArXiv e-prints*
 Blakeslee J. P., Cho H., Peng E. W., Ferrarese L., Jordán A., Martel A. R., 2012, *ApJ*, 746, 88
 Bovy J., Rix H.-W., Hogg D. W., Beers T. C., Lee Y. S., Zhang L., 2012a, *ApJ*, 755, 115
 Bovy J., Rix H.-W., Liu C., Hogg D. W., Beers T. C., Lee Y. S., 2012b, *ApJ*, 753, 148
 Boylan-Kolchin M., Springel V., White S. D. M., Jenkins A., 2010, *MNRAS*, 406, 896
 Brodie J. P., Strader J., 2006, *ARA&A*, 44, 193
 Brogaard K. et al., 2012, *A&A*, 543, A106
 Brown J. A., Wallerstein G., Zucker D., 1997, *AJ*, 114, 180
 Carrera R., Gallart C., Aparicio A., Costa E., Méndez R. A., Noël N. E. D., 2008a, *AJ*, 136, 1039
 Carrera R., Gallart C., Hardy E., Aparicio A., Zinn R., 2008b, *AJ*, 135, 836
 Carretta E., Bragaglia A., Gratton R., D’Orazi V., Lucatello S., 2009a, *A&A*, 508, 695
 Carretta E., Bragaglia A., Gratton R., Lucatello S., 2009b, *A&A*, 505, 139
 Casagrande L., Schönrich R., Asplund M., Cassisi S., Ramírez I., Meléndez J., Bensby T., Feltzing S., 2011, *A&A*, 530, A138
 Casetti-Dinescu D. I., Girard T. M., Herrera D., van Altena W. F., López C. E., Castillo D. J., 2007, *AJ*, 134, 195
 Casetti-Dinescu D. I., Girard T. M., Jílková L., van Altena W. F., Podestá F., López C. E., 2013, *AJ*, 146, 33
 Cohen J. G., 2004, *AJ*, 127, 1545
 Cole A. A., Tolstoy E., Gallagher, III J. S., Smecker-Hane T. A., 2005, *AJ*, 129, 1465
 Colucci J. E., Bernstein R. A., Cameron S. A., McWilliam A., 2011, *ApJ*, 735, 55
 Cooper A. P. et al., 2010, *MNRAS*, 406, 744
 Cooper A. P., D’Souza R., Kauffmann G., Wang J., Boylan-Kolchin M., Guo Q., Frenk C. S., White S. D. M., 2013, *MNRAS*
 Cote P., Marzke R. O., West M. J., 1998, *ApJ*, 501, 554
 De Angeli F., Piotto G., Cassisi S., Busso G., Recio-Blanco A., Salaris M., Aparicio A., Rosenberg A., 2005, *AJ*, 130, 116
 Deason A. J., Belokurov V., Evans N. W., 2011, *MNRAS*, 416, 2903
 Deason A. J. et al., 2012, *MNRAS*, 425, 2840
 Dinescu D. I., Girard T. M., van Altena W. F., 1999, *AJ*, 117, 1792
 Dinescu D. I., Girard T. M., van Altena W. F., López C. E., 2003, *AJ*, 125, 1373
 Dotter A., Sarajedini A., Anderson J., 2011, *ApJ*, 738, 74
 Eggen O. J., Lynden-Bell D., Sandage A. R., 1962, *ApJ*, 136, 748
 Elmegreen B. G., Malhotra S., Rhoads J., 2012, *ApJ*, 757, 9
 Forbes D. A., Bridges T., 2010, *MNRAS*, 404, 1203
 Forbes D. A., Brodie J. P., Grillmair C. J., 1997, *AJ*, 113, 1652
 Furukawa N., Dawson J. R., Ohama A., Kawamura A., Mizuno N., Onishi T., Fukui Y., 2009, *ApJL*, 696, L115
 Gallazzi A., Charlot S., Brinchmann J., White S. D. M., Tremonti C. A., 2005, *MNRAS*, 362, 41
 Gilmore G., Wyse R. F. G., 1998, *AJ*, 116, 748
 Giocoli C., Pieri L., Tormen G., 2008, *MNRAS*, 387, 689
 Glatt K. et al., 2008, *AJ*, 136, 1703
 Gratton R. G., Carretta E., Bragaglia A., 2012, *A&ARv*, 20, 50
 Gratton R. G., Carretta E., Bragaglia A., Lucatello S., D’Orazi V., 2010, *A&A*, 517, A81
 Guo Q., White S., Li C., Boylan-Kolchin M., 2010, *MNRAS*, 404, 1111
 Harris W. E., 2010, *ArXiv e-prints*
 Hartwick F. D. A., 2009, *ApJ*, 691, 1248
 Hill V., 1997, *A&A*, 324, 435
 Jurić M. et al., 2008, *ApJ*, 673, 864
 Karim A. et al., 2011, *ApJ*, 730, 61
 Keller S. C., Mackey D., Da Costa G. S., 2012, *ApJ*, 744, 57
 Kirby E. N., Lanfranchi G. A., Simon J. D., Cohen J. G., Guhathakurta P., 2011, *ApJ*, 727, 78
 Larsen S. S., Brodie J. P., Huchra J. P., Forbes D. A., Grillmair C. J., 2001, *AJ*, 121, 2974
 Law D. R., Majewski S. R., 2010, *ApJ*, 718, 1128
 Leaman R., 2012, *AJ*, 144, 183
 Leaman R., Cole A. A., Venn K. A., Tolstoy E., Irwin M. J., Szeifert T., Skillman E. D., McConnachie A. W., 2009, *ApJ*, 699, 1
 Leaman R. et al., 2013, *ApJ*, 767, 131
 Leaman R. et al., 2012, *ApJ*, 750, 33
 Leauthaud A. et al., 2012, *ApJ*, 744, 159
 Lee H., Bell E. F., Somerville R. S., 2008, in *IAU Symposium*, Vol. 255, IAU Symposium, Hunt L. K., Madden S. C., Schneider R., eds., pp. 100–105
 Lee H., Skillman E. D., Cannon J. M., Jackson D. C., Gehrz R. D., Polonski E. F., Woodward C. E., 2006, *ApJ*, 647, 970
 Letarte B., Hill V., Jablonka P., Tolstoy E., François P., Meylan G., 2006, *A&A*, 453, 547
 Mackey A. D. et al., 2013, *MNRAS*, 429, 281
 Mackey A. D., van den Bergh S., 2005, *MNRAS*, 360, 631
 Marín-Franch A. et al., 2009, *ApJ*, 694, 1498
 Mateluna R., Geisler D., Villanova S., Carraro G., Grochol-

- ski A., Sarajedini A., Cole A., Smith V., 2012, *A&A*, 548, A82
- Mateo M. L., 1998, *ARA&A*, 36, 435
- McConnachie A. W., 2012, *AJ*, 144, 4
- McMillan P. J., 2011, *MNRAS*, 414, 2446
- Meidt S. E. et al., 2013, *ArXiv e-prints*
- Morrison H. L., 1993, *AJ*, 106, 578
- Mottini M., Wallerstein G., McWilliam A., 2008, *AJ*, 136, 614
- Mucciarelli A. et al., 2011, *MNRAS*, 413, 837
- Muratov A. L., Gnedin O. Y., 2010, *ApJ*, 718, 1266
- Nordström B. et al., 2004, *A&A*, 418, 989
- Parisi M. C., Geisler D., Grocholski A. J., Clariá J. J., Sarajedini A., 2010, *AJ*, 139, 1168
- Peng E. W. et al., 2008, *ApJ*, 681, 197
- Pompéia L. et al., 2008, *A&A*, 480, 379
- Pota V. et al., 2013, *MNRAS*, 428, 389
- Pritzl B. J., Venn K. A., Irwin M., 2005, *AJ*, 130, 2140
- Rix H.-W., Bovy J., 2013, *A&ARv*, 21, 61
- Robin A. C., Reylé C., Derrière S., Picaud S., 2003, *A&A*, 409, 523
- Rosenberg A., Saviane I., Piotto G., Aparicio A., 1999, *AJ*, 118, 2306
- Roškar R., Debattista V. P., Quinn T. R., Stinson G. S., Wadsley J., 2008, *ApJL*, 684, L79
- Sarajedini A. et al., 2007, *AJ*, 133, 1658
- Saviane I., da Costa G. S., Held E. V., Sommariva V., Gullieuszik M., Barbuy B., Ortolani S., 2012, *A&A*, 540, A27
- Schlegel D. J., Finkbeiner D. P., Davis M., 1998, *ApJ*, 500, 525
- Schönrich R., Asplund M., Casagrande L., 2011, *MNRAS*, 415, 3807
- Searle L., Zinn R., 1978, *ApJ*, 225, 357
- Sellwood J. A., Binney J. J., 2002, *MNRAS*, 336, 785
- Smecker-Hane T. A., McWilliam A., 2002, *ArXiv Astrophysics e-prints*
- Spitler L. R., Forbes D. A., 2009, *MNRAS*, 392, L1
- Strader J., Brodie J. P., Cenarro A. J., Beasley M. A., Forbes D. A., 2005, *AJ*, 130, 1315
- Strader J., Brodie J. P., Forbes D. A., 2004, *AJ*, 127, 3431
- Tautvaišienė G., Wallerstein G., Geisler D., Gonzalez G., Charbonnel C., 2004, *AJ*, 127, 373
- Tremonti C. A. et al., 2004, *ApJ*, 613, 898
- Unavane M., Wyse R. F. G., Gilmore G., 1996, *MNRAS*, 278, 727
- van den Bergh S., 2000, *ApJ*, 530, 777
- van den Bosch F. C., Lewis G. F., Lake G., Stadel J., 1999, *ApJ*, 515, 50
- VandenBerg D. A., 2000, *ApJS*, 129, 315
- VandenBerg D. A., Brogaard K., Leaman R., Casagrande L. V., 2013, *ApJ* (in press)
- Venn K. A., Irwin M., Shetrone M. D., Tout C. A., Hill V., Tolstoy E., 2004, *AJ*, 128, 1177
- Vera-Ciro C. A., Helmi A., Starkenburg E., Breddels M. A., 2013, *MNRAS*, 428, 1696
- Wang J. et al., 2011, *MNRAS*, 413, 1373
- Yoon S.-J. et al., 2011, *ApJ*, 743, 150
- Zahid H. J., Geller M. J., Kewley L. J., Hwang H. S., Fabricant D. G., Kurtz M. J., 2013, *ApJL*, 771, L19
- Zhao H., 2004, *MNRAS*, 351, 891
- Zolotov A., Willman B., Brooks A. M., Governato F., Brook C. B., Hogg D. W., Quinn T., Stinson G., 2009, *ApJ*, 702, 1058